

URA Visiting Scholars Program: Project Proposal

Gleb Lukicov
University College London

August 23, 2018

1 Project description

1.1 Overview

The muon magnetic dipole moment is related [1] to its intrinsic spin, \mathbf{s} , by the relation

$$\boldsymbol{\mu} = g_\mu \left(\frac{e}{2m_\mu} \right) \mathbf{s}, \quad (1)$$

where g_μ defines the gyromagnetic ratio of the muon. g_μ encompasses the interaction of the muon with the magnetic field, and the nature of these interactions changes g_μ . The anomalous magnetic moment, a_μ , is the net effect of these interactions beyond the Dirac interaction, and is given by

$$a_\mu = \frac{g_\mu - 2}{2}. \quad (2)$$

The current theoretical prediction [2] of a_μ is $0.00116591817(42)$, with a precision of 360 ppb (parts per billion), which comprises numerous contributions from electromagnetic, electroweak, and hadronic interactions. This accuracy is comparable to the experimental accuracy of the previous Muon g-2 experiment at Brookhaven (E821) [3], which had a result of $0.00116592091(63)$, with a precision of 540 ppb. The difference between the E821 experiment and theory corresponds to a 3.6σ deviation between the experiment and the theory. To account for this discrepancy, a Beyond Standard Model (BSM) correction to α_μ may be required. This provides a clear motivation for a more precise measurement of the a_μ .

1.2 The Muon g-2 Experiment at Fermilab

The Fermilab g-2 experiment (E989) [4] will determine the a_μ to a precision of 140 ppb, which would correspond to a 7σ deviation between the experiment and the theory, provided that the central values of the measurement and prediction do not change. The g-2 experiment has successfully completed its first data taking period (Run 1) between January 2018 and July 2018, with Run 2 commencing in October 2018. Achieving the experimental goal requires a dataset containing 1.5×10^{11} positrons with energy above 1.8 GeV which will be accumulated over the next two years. The momentum of the injected muons is 3.09 GeV: the so-called “magic momentum” at which the motional magnetic field is zero. The actual measurement performed is of the anomalous precession frequency (ω_a), and the strength of the applied magnetic field (\mathbf{B}), which is also a frequency measurement determined using Nuclear Magnetic Resonance (NMR).

Longitudinally polarised muons are injected into the storage ring (see Fig. 1), where they follow a circular orbit in a magnetic dipole field \mathbf{B} and a vertically focusing electric quadrupole field \mathbf{E} . The muon beam passes through an inflector magnet which provides a cancellation of the magnetic field in that region, to allow the beam to enter the storage ring without deflection. This requirement on the inflector means that the beam is injected at a 1.25° angle, displacing the actual orbit by 77 mm radially outward from the closed orbit. This is adjusted by the fast muon kicker, which is a pulsed magnet with a vertical magnetic field that



Fig. 1. The E989 storage ring at Fermilab, which was originally designed for the E821 experiment. Superconducting magnets provide a uniform radial magnetic dipole field of 1.45 T. The 24 calorimeters are shown distributed uniformly on the inside of the ring. The beam (shown in red at the top of the figure) enters the storage ring via the inflector. The direction of the beam is clockwise in this orientation.

directs the muons onto the closed orbit.

The spin of a muon precesses around the momentum vector, which follows the closed circular orbit. Due to the $V - A$ structure of the weak interaction, the highest energy positrons are emitted along the direction of the spin of the decaying muons (in the rest frame of the muon), while neutrinos are emitted anti-parallel with respect to the muon spin ($\mu^+ \rightarrow e^+ \nu_e \bar{\nu}_\mu$). The decay positrons have a lower energy than the original muons, as a result, positrons curl inwards (towards the centre of the ring) and are detected in 24 calorimeters on the inside of the storage ring.

The anomalous precession frequency, ω_a , is determined by a_μ and the strength of the magnetic field via

$$\omega_a = -a_\mu \frac{e}{m_\mu} \mathbf{B} = -\left(\frac{g-2}{2}\right) \frac{e}{m_\mu} \mathbf{B}. \quad (3)$$

The second frequency measurement in the experiment is that of ω_p , the Larmor frequency of a free proton, which is measured by NMR probes to establish the magnetic flux density ($|\mathbf{B}|$)

$$\omega_p = \gamma_p |\mathbf{B}|, \quad (4)$$

where $\gamma_p = 2.675222005(63) \times 10^8 \text{ s}^{-1} \cdot \text{T}^{-1}$ [5] is the free proton gyromagnetic moment ratio. The a_μ is then determined from the two frequencies and the muon-to-proton magnetic moment ratio

$$a_\mu = \frac{\omega_a / \omega_p}{\mu_\mu / \mu_p - \omega_a / \omega_p} = \frac{\omega_a}{\omega_p} \left(\frac{g_e}{2}\right) \left(\frac{m_\mu}{m_e}\right) \left(\frac{\mu_p}{\mu_e}\right). \quad (5)$$

Beam dynamics effects such as the momentum spread (away from the “magic momentum”), Δp , and Coherent Betatron Oscillation (CBO) [6] contribute significantly to the systematic uncertainty on ω_a : at 30 ppb each. Since the calorimeter acceptance for the decay positron depends on the radial coordinate of the muon at the point where it decays, CBO of the stored beam can produce an amplitude modulation in the observed positron time spectrum. Therefore, it is necessary to monitor these effects with a sensitive detector system, such as a tracking detector. Moreover, the largest single systematic uncertainty (40 ppb) associated with the calorimeters is pileup, which occurs when, for example, two low energy positrons deposit energy in the same crystal within the measurement time window ($\sim 5 \text{ ns}$). The pileup can be resolved by the tracking detector, which would reconstruct two independent trajectories for the two low energy positrons.

1.3 Tracking Detector

The tracking detector [7] (shown in Fig. 2) registers the trajectory of the positrons from the μ^+ decay in the storage ring. The two adjacent straw planes (*doublets*) are oriented at a 7.5° stereo angle relative to the other doublet - to provide a 2D position from a hit. A 3D trajectory is reconstructed by extrapolating across all modules. Each aluminised mylar straw is $15\ \mu\text{m}$ thick, and is held at 1 atm pressure. The tracker measures the muon spatial distribution (shown in Fig. 3.a), which must be convoluted with the measured magnetic field map in the storage region to determine the effective field seen by the muon beam. Moreover, particle identification can be achieved by combining calorimeter information with that from the tracker (see Fig. 3.b).

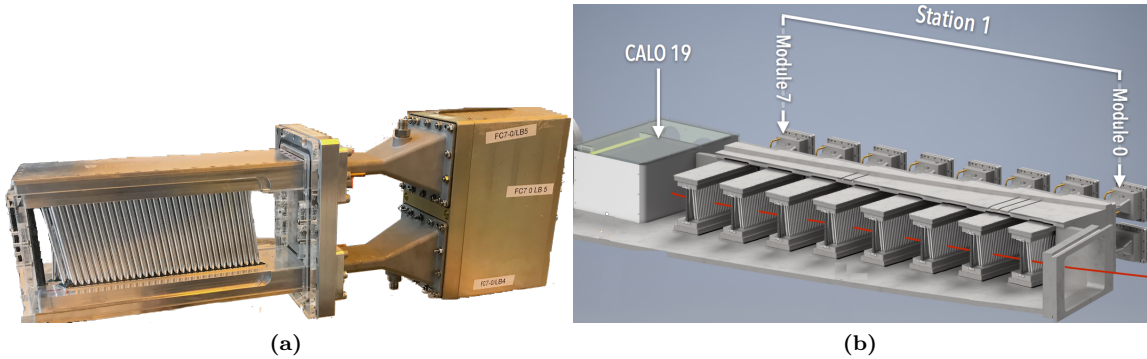


Fig. 2. (a) A single tracker module with the Front-end Low Voltage Optical Box to Back-end Readout (FLOBBER): one of the 4 rows of 32 straws is shown, which are held between two manifolds. A straw (length=100 mm, diameter=5 mm) is an ionisation chamber filled with 50:50 Ar:Ethane, with a central cathode wire at $+1.6\ \text{kV}$. The active tracking region is inside the storage ring vacuum ($\sim 10^{-9}\ \text{atm}$) and the readout fibre cables bring the data upstream from the FLOBBER to the DAQ system. (b) Rendering of a simulated decay positron trajectory passing through the trackers before hitting the calorimeter.

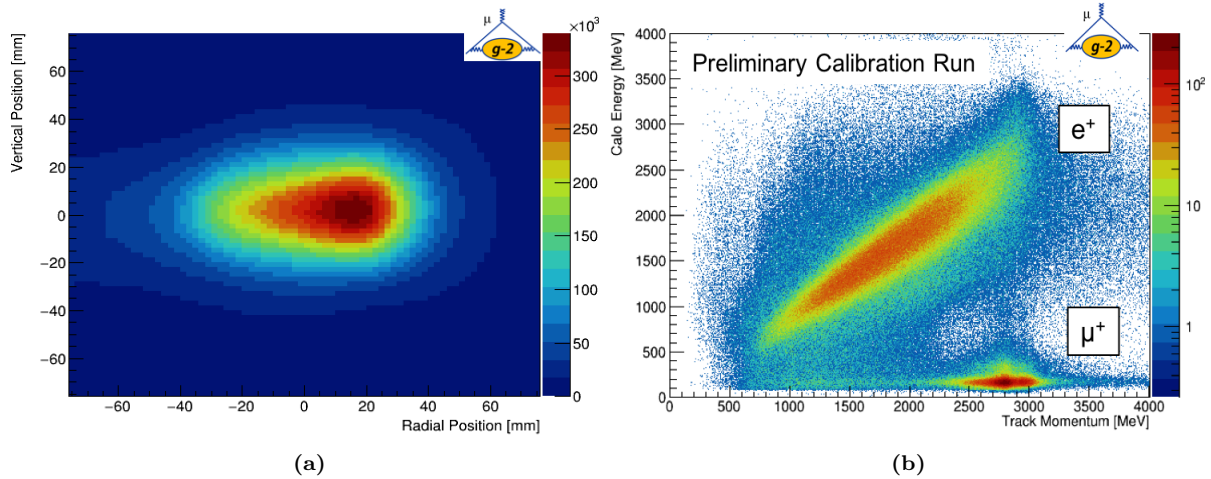


Fig. 3. (a) Reconstructed radial and vertical beam position from tracks that have been extrapolated back to their decay position. (b) Comparing the measured tracker momentum and calorimeter energy shows two distinct populations - positrons that are mostly contained in the calorimeter, and high momentum lost muons which only deposit a small amount of energy in the calorimeter.

Additionally, the tracker can realise an Electric Dipole Moment (EDM) measurement through the vertical asymmetry of the muon decay, which changes the observed precession frequency by an additional frequency due to the EDM. The goal is to place a new limit on the muon EDM, with a sensitivity of $1.8 \times 10^{-21}\ \text{e}\cdot\text{cm}$, a 100 fold improvement on the Brookhaven result [8].

In order for the tracking detector to reduce the systematic uncertainty on the a_μ measurement and improve the sensitivity to a muon EDM, the absolute position of the tracking modules must be known to a high level of precision. Individual straw effects such as reduced wire tension, can affect different straws in a different way. Therefore, a physics-level (i.e. track-based) alignment, that considers such effects, is required. Track-based alignment will be implemented with data from Run 1 using the **Millepede II** framework [9]. A Monte Carlo (MC) simulation was developed to understand the detector geometry and how this affects how well the alignment can be determined, as well as to test the alignment procedure itself (see Fig. 4). This could potentially be the largest current improvement to the tracking algorithms. The beam extrapolation (as shown in Fig. 3.b) will also greatly benefit from the internal alignment of the tracker.

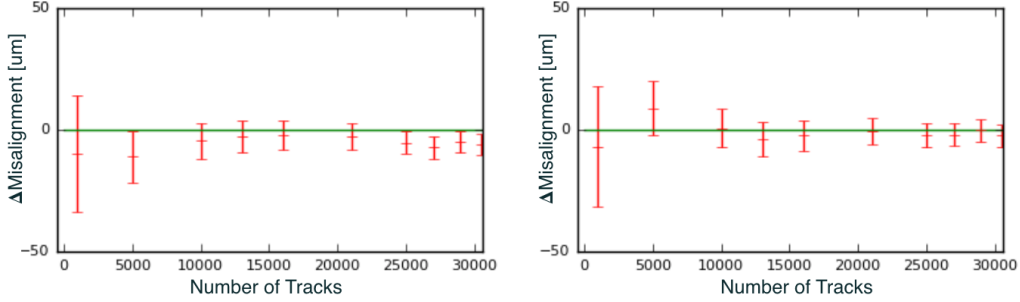


Fig. 4. Figure of Merit: The difference in vertical misalignment between the simulation input and the Millepede II prediction vs. the number of generated tracks in 2 modules.

1.4 DAQ

An essential component of the experiment is the Data acquisition (DAQ) system [10], which manages the data flow from the detector electronics. The experiment is acquiring raw data at a rate of 20 GB/s. This is accomplished by employing parallel data-processing architecture using 28 high-speed GPUs (NVIDIA *Tesla K40*) to process data from 12 bit waveform digitisers, reducing the recorded data rate to 200 MB/s. The set-up is controlled by the MIDAS [11] software framework. The system processes data from 1296 calorimeter channels, 2 straw tracker stations, and auxiliary detectors (e.g. entrance μ counters). The total data output of the experiment to tape during Run 1 was 2 PB. Additionally, a PCI-based GPS synchronisation card is used to GPS-timestamp the digitised data in order to facilitate subsequent matching between the detector system readout and the magnetic field readout

An event display (see Fig. 5) that uses Visualization Toolkit (VTK) to display hits on calorimeters have been developed by the Dubna group for the experiment, and its installation will be taking place during the 2018 shutdown. The maintenance of the event display will be an important task for the near real time data quality monitoring during Run 2.

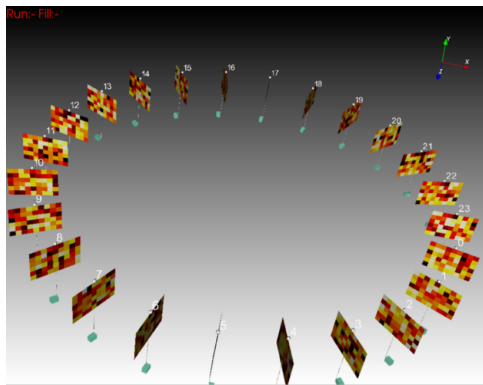


Fig. 5. VTK based event display GUI: application connects to the DAQ system to retrieve hit information in near real time.

The DAQ system performed admirably during Run 1 with 90% uptime, with nearly twice the amount of collected data compared to the E821 experiment (as shown in Fig.6). The most common cause of downtime was due to a dropped 10 GB fibre link from a digitiser to a PC, which causes the buffers to overfill. This is currently being addressed during the shutdown, and a continuous DAQ system improvement effort will continue during Run 2 and beyond.

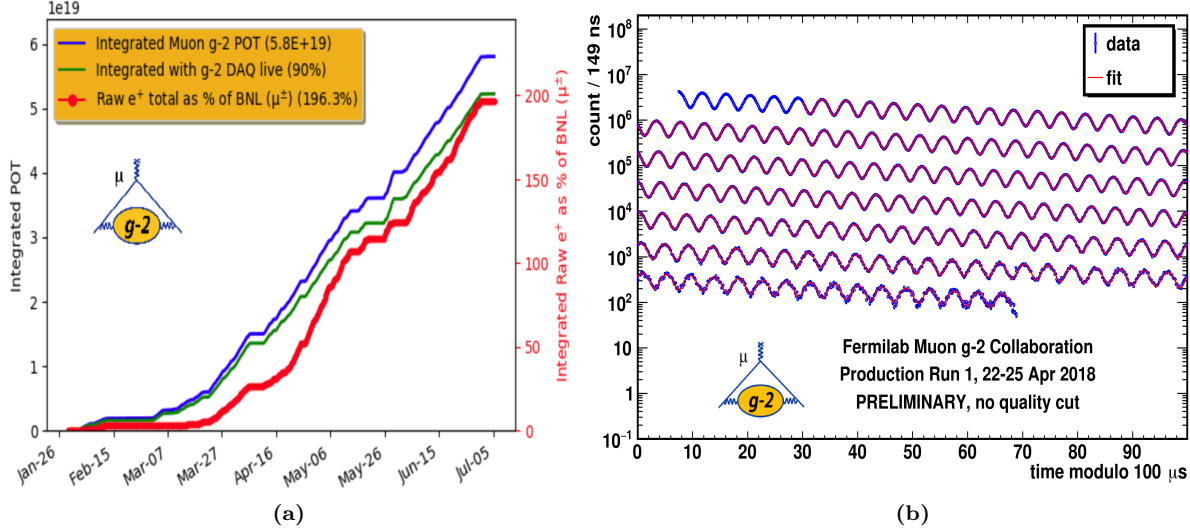


Fig. 6. (a) Integrated protons on target (POT) delivered to the g-2 experiment during Run 1 and the total data collected. (b) Histogram, modulo 100 μs , of 0.95 billion collected positrons. Data (in blue) was summed over all calorimeters, with a least-squares fit (in red). ω_a is extracted from the data as one of the fit parameters. This figure was accumulated from 60 hours of data from 22 - 25 Apr 2018, a similar data size to the one achieved by E821 experiment in 1999.

2 Proposed Research Activity at Fermilab

I have developed and tested alignment algorithms that are fully integrated with the existing tracking *art* [12] framework (see Fig. 7). My immediate goal is to start utilising the alignment framework with the Run 1 data to improve the internal alignment of the tracking detector. The subsequent task is to continue to improve the alignment of the detector after a transient effect, such as a sudden change in the ring vacuum pressure or a module swap, by continuously running the alignment routine on a subset of data and writing the alignment (calibration) constants ($\sim 12,000$ alignment parameters) into a database. The final estimation of the overall alignment capability of the detector will require correlation of the track-based alignment and the survey-based alignment, which is being performed by the Fermilab team.

During Run 1, I have trained in my role as a DAQ expert and performed on-call duties for the tracker and calorimeter DAQ and data quality monitoring systems, and have participated in the installation and commissioning of the tracking detector and the DAQ. For the upcoming run, I hope to continue in my role as a DAQ expert on-call, as it provides me with unique practical learning opportunities not available elsewhere. I aspire to direct my future scientific career to focus on hardware and electronics R&D, and being part of the on-site DAQ team gives me the essential exposure to the modern data readout and storage technologies.

One of my current tasks involves integration of the event display with the DAQ system of the experiment. Over the course of Run 2, I will be responsible for maintaining and improving the event display infrastructure, which ideally requires an on-site presence. Moreover, as the analysis of the Run 1 data is gaining more momentum, a new critical area of activity is emerging - data quality control. Being on-site at Fermilab during Run 2 will give me the maximum benefit of being able to contribute to this important work.

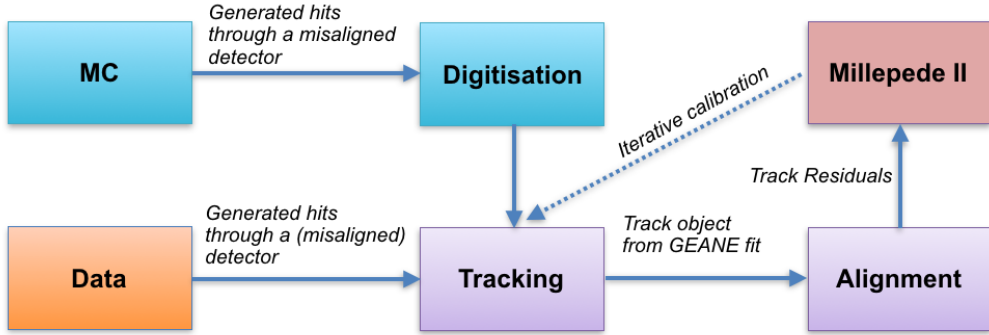


Fig. 7. The software framework of the alignment chain.

3 Summary

Improvement of the tracking algorithms is essential in order to realise the systematic goals of the experiment. The URA Visiting Scholars Program scholarship will allow me to maximally contribute to the development of such algorithms, as well as to contribute to the tracker team to maintain and operate the tracking detector. Liaising with the Fermilab survey alignment team will be an important task for me in order to correlate the final alignment results. Moreover, the scholarship will allow me to continue in my essential role as a member of the DAQ expert on-call team. As Run 2 will see an increased amount of data flow, a near instant event display will be crucial to monitor the quality of the data, and I will be the only team member on-site that will oversee the maintenance of the event display. Finally, there is an opportunity to contribute to the data quality control development, which provides a unique learning opportunity to relate hardware performance with the analysis campaign.

This proposal is supported by my faculty adviser Prof. Mark Lancaster (m.lancaster@ucl.ac.uk) and Fermilab collaborator Brendan Casey (bcasey@fnal.gov).

References

- [1] B. Roberts, Y. Semertzidis, *Lepton Dipole Moments*, World Scientific, Singapore (2010).
- [2] M. Davier, *Update of the Hadronic Vacuum Polarisation Contribution to the Muon g-2*, Nucl. Part. Phys. Proc. **287**, 70 (2017).
- [3] G. Bennett et al., *Final Report of the Muon E821 Anomalous Magnetic Moment Measurement at BNL*, Phys. Rev. D **73**, 072003 (2006).
- [4] J. Grange et al., *Muon (g-2) Technical Design Report*, arXiv:1501.06858 (2015).
- [5] P. Mohr, B. Taylor, and D. Newell, *CODATA: Recommended Values of the Fundamental Physical Constants*, Rev. Mod. Phys. **84**, 1527 (2012).
- [6] Y. Srivastava, and A. Widom, *Coherent Betatron Oscillation and Induced Errors in the Experimental Determination of the Muon g-2 Factor*, arXiv:hep-ph/0109020 (2001).
- [7] T. Stuttard, *The Development, Testing and Characterisation of a Straw Tracking Detector and Readout System for the Fermilab Muon g-2 Experiment*, PhD thesis, University College London (2017).
- [8] G. Bennett et al., *Improved Limit on the Muon Electric Dipole Moment*, Phys. Rev. D **80**, 052008 (2009).
- [9] V. Blobel *Software Alignment for Tracking Detectors*, Nucl. Instrum. Methods A, **556**, 5 (2006).
- [10] W. Gohn, *Data Acquisition for the New Muon g-2 Experiment at Fermilab*, J. Phys. **664**, 8 (2015).
- [11] *MIDAS documentation*, (TRIUMF, PSI), https://midas.triumf.ca/MidasWiki/index.php/Midas_documentation (2015).
- [12] C. Green et al., *The Art Framework*, J. Phys. Conf. Ser. **396**, 022020 (2012).